CIRCULAR CYLINDRICAL DIELECTRIC-COATED METAL ROD EXCITED IN THE SYMMETRIC TM$_{01}$ MODE

Part II. Radiation Characteristics

By R. Chatterjee and T. Chandrakaladhara Rao*

(Department of Electrical Communication Engineering, Indian Institute of Science, Bangalore-12, India)

Abstract

The radiation pattern of a dielectric-coated metal cylinder is theoretically derived by applying Schelkunoff's Equivalence Principle. The radiation characteristics of the antenna like the position and beam width of the major lobe, positions and intensities of sidelobes and the gain are determined and their variations with the physical parameters of the antenna like the length (1), the b/a ratio, the conductor radius (a), the dielectric constant (ϵ_r) and the frequency of excitation (f). Some of the theoretical results have been verified by experiments.

1. Introduction

The problem of radiation from surface wave structures has been studied by several investigators[1-14]. Different kinds of theoretical approaches have been attempted to explain the observed experimental radiation patterns. Schelkunoff's Equivalence Principle[1, 3, 4, 5, 7, 8], Aperture theory[6, 9], Lens approach[2], and Vector Kirchhoff formula[11, 12] have yielded results which showed reasonable agreement with the experiment. An excellent review of the various approaches attempted till 1952 appears in the form of a monograph by Kiely[10]. James[11] examined the mathematical validity of the existing theoretical approaches and made a critical analysis of them.

In this paper, we propose to study the surface wave radiation characteristics of a circular cylindrical dielectric-coated metal roh excited in the ' TM$_{01}$' mode. The method of approach is by the application of Schelkunoff's equivalence principle.

* At present with the Special Projects Team, Hindustan Aeronautics, Ltd., Hyderabad Division, Hyderabad-42.

2. Schelkunoff's Equivalence Principle

The equivalence principle states that the electromagnetic field inside a closed surface Σ due to sources outside the surface can be produced by an equivalent sheet electric current $\vec{J}$ and a sheet magnetic current $\vec{M}$ distributed over Σ and related to the electric and magnetic fields $\vec{E}_0$ and $\vec{H}_0$ by the relations

$$\vec{J} = \vec{n} \times \vec{H}_0$$

$$\vec{M} = -\vec{n} \times \vec{E}_0 \tag{2.1}$$

where $\vec{E}_0$ and $\vec{H}_0$ represent the values of the electric and magnetic fields on the surface Σ and $\vec{n}$ is the unit normal vector directed outwards from Σ.

The electric and magnetic vector potentials $\vec{A^E}$ and $\vec{A^H}$ at a point P within Σ are related to these equivalent currents through the relations,

$$\left.\begin{aligned}
\vec{A^E} &= \frac{1}{4\pi} \iint_{\Sigma} \frac{\vec{M} \exp j(\omega t - kr_1)}{r_1} \, d\Sigma \\
\vec{A^H} &= \frac{1}{4\pi} \iint_{\Sigma} \frac{\vec{J} \exp j(\omega t - kr_1)}{r_1} \, d\Sigma
\end{aligned}\right\} \tag{2.2}$$

where ' r_1 ' is the distance between an elemental surface ' $d\Sigma$ ' on Σ and the point P. $k = 2\pi/\lambda_0$ is the free space wavenumber while ' λ_0 ' is the free space wavelength. A time dependance of exp $(j\omega t)$ is assumed.

The electric and magnetic fields $\vec{E}_P$ and $\vec{H}_P$ respectively at the point P are then given by

$$\left.\begin{aligned}
\vec{E}_P &= -j\omega\mu_0 \vec{A^H} + \frac{1}{j\omega\epsilon_0} \operatorname{grad} \operatorname{div} \vec{A^H} - \operatorname{curl} \vec{A^E} \\
\\
\vec{H}_P &= -j\omega\epsilon_0 \vec{A^E} + \frac{1}{j\omega\mu_0} \operatorname{grad} \operatorname{div} \vec{A^E} + \operatorname{curl} \vec{A^H}
\end{aligned}\right\} \tag{2.3}$$

and

These equations are utilized to find the far field radiation pattern of the dielectric-coated conducting cylindrical rod. The sources are distributed in the three regions (see Fig. 1).
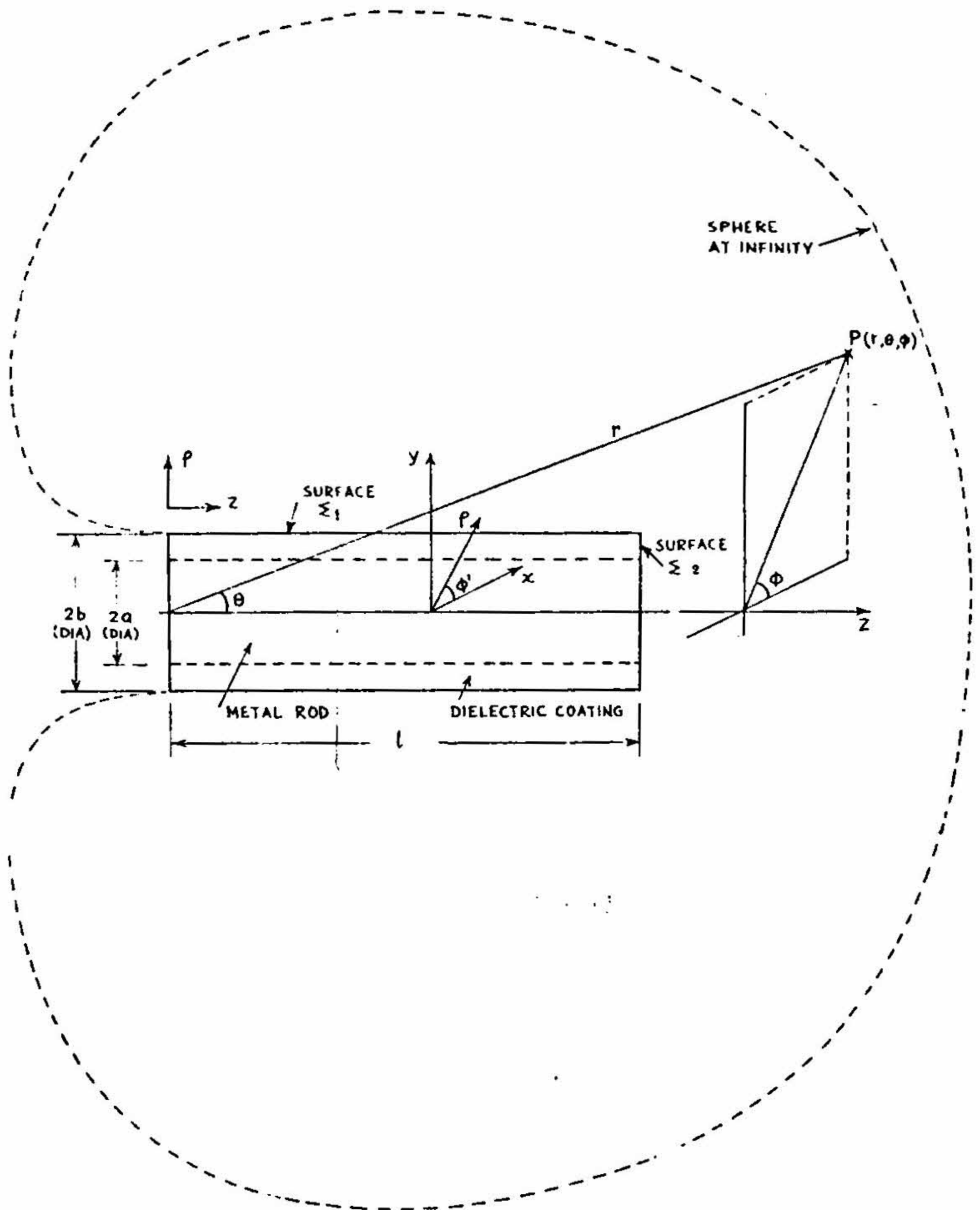

FIG. 1 Surfaces of integration to calculate the radiated field.

(i) The cylindrical dielectric surface of the rod

$$\Sigma_1 = \int_0^l \int_{\phi'=0}^{2\pi} b\,d\phi'\,dz.$$

(2.4)

(ii) Free end of the rod

$$\Sigma_2 = \int_{\phi'=0}^{2\pi} \int_{\rho=0}^{b} \rho\,d\rho\,d\phi'.$$

(2.5)

where 'l' is the length of the antenna.

(iii) Σ_3 includes the outer surface of the mode transducer and a sphere of a very large radius, on which the currents are negligible.

3. FIELD COMPONENTS

The field components in the region of the dielectric coating $[a \leqslant \rho \leqslant b]$ are[14]

$$E_z = -\frac{A\left[J_0\left(\frac{h\rho}{b}\right)Y_0(u) - J_0(u)Y_0\left(\frac{h\rho}{b}\right)\right]}{Y_0(u)}\exp(-j\beta z)$$

$$\left. \begin{array}{l} H_{\phi'} = -\dfrac{j\omega\epsilon_1 b}{h}\dfrac{A\left[J_0'\left(\frac{h\rho}{b}\right)Y_0(u) - J_0(u)Y_0'\left(\frac{h\rho}{b}\right)\right]}{Y_0(u)}\exp(-j\beta z) \\[4mm] E_{\rho} = -\dfrac{j\beta b}{h}\dfrac{A\left[J_0'\left(\frac{h\rho}{b}\right)Y_0(u) - J_0(u)Y_0'\left(\frac{h\rho}{b}\right)\right]}{Y_0(u)}\exp(-j\beta z) \end{array} \right\}$$

(3.1)

4. DERIVATION OF THE FAR-FIELD RADIATION PATTERN

As mentioned earlier, the contribution for the radiation field arises from three different regions, *viz.*, Σ_1, Σ_2 and Σ_3.

4.1. *Contribution from the Cylindrical Dielectric Surface* (Σ_1)

While considering the contribution from this surface, the two tangential field components of interest are E_z and $H_{\phi'}$. These two components exist and have values given below at the surface $\rho = b$.

$$\left. \begin{array}{l} E_z = A[P(h)/Y_0(u)]\exp(-j\beta z) = C_1\exp(-j\beta z) \\[3mm] H_{\phi'} = \left(\dfrac{-j\omega\epsilon_1 b}{h}\right)A\left[\dfrac{P'(h)}{Y_0(u)}\right]\exp(-j\beta z) \end{array} \right\}$$

(4.1)

$$= C_2\exp(-j\beta z)$$

where

$$P(h) = J_0(h) Y_0(u) - J_0(u) Y_0(h) \\
P'(h) = J_0'(h) Y_0(u) - J_0(u) Y_0'(h) \Big\} \tag{4.2}$$

The unit vector perpendicular to the surface under consideration is in the ρ-direction. Applying the definitions of $\vec{J}$ and $\vec{M}$

$$\vec{J} = \vec{\rho} \times \vec{\phi'} H_{\phi'} = \vec{z} J_z$$

$$= \vec{z} \left\{ \frac{-j\omega\epsilon_1 b}{h} A \frac{P'(h)}{Y_0(u)} \right\} \exp(-j\beta z)$$

and

$$\vec{M} = -\vec{\rho} \times \vec{z} E_z = \vec{\phi'} M_{\phi'}$$

$$= \vec{\phi'} \left\{ \frac{AP(h)}{Y_0(u)} \right\} \exp(-j\beta z) \tag{4.3}$$

Using the transformations given in Table I equations (4.3) can be simplified.

Hence

$$\vec{J} = \{\vec{r}(\cos\theta) + \vec{\theta}(-\sin\theta)\} \left\{ \frac{-j\omega\epsilon_1 b}{h} A \frac{P'(h)}{Y_0(u)} \right\}$$

$$\times \exp(-j\beta z)$$

$$\vec{M} = [\vec{r}(-\sin\theta\sin\overline{\phi'-\phi}) + \vec{\theta}(-\cos\theta\sin\overline{\phi'-\phi})$$

$$+ \vec{\phi}(\cos\overline{\phi'-\phi})] \left[A \frac{P(h)}{Y_0(u)} \right] \exp(-j\beta z) \tag{4.4}$$

The distance 'r_1' between an element of area $d\Sigma_1 = b d\phi' dZ$ on the cylindrical dielectric surface and an external point $P(r, \theta, \phi)$ is

$$r_1 = r - b\sin\theta\cos(\phi' - \phi) - z\cos\theta \tag{4.5}$$

which may be approximated by

$$r_1 = r \text{ in the amplitude terms.}$$

If $d\vec{A^H}$, $d\vec{A^E}$ represent the vector potentials at the point $P(r, \theta, \phi)$ due to the surface element $d\Sigma_1$, then the vector potentials due to the complete surface of the dielectric-coated conducting cylinder are given by

$$\vec{A^H} = \int_{z=0}^{l} \int_{\phi'=0}^{2\pi} d\vec{A^H}$$

$$= \int_{z=0}^{l} \int_{\phi'=0}^{2\pi} \frac{\vec{J} \exp j(\omega t - kr_1)}{4\pi r_1} d\Sigma_1 \qquad (4.6\,a)$$

and similarly

$$\vec{A^E} = \int_{z=0}^{l} \int_{\phi'=0}^{2\pi} \frac{\vec{M} \exp j(\omega t - kr_1)}{4\pi r_1} d\Sigma_1 \qquad (4.6\,b)$$

where l = length of the antenna and

$$d\Sigma_1 = b d\phi' dz.$$

The electric field at the distant point is then given by

$$\vec{E_P} = \int_{z=0}^{l} \int_{\phi'=0}^{2\pi} \Big[-j\omega\mu_0 d\vec{A^H} + \frac{1}{j\omega\epsilon_0} \text{ grad div } \vec{A^H}$$

$$- \text{curl } d\vec{A^E} \Big] d\Sigma_1. \qquad (4.7)$$

Transforming the gradient, divergence and the curl operations to spherical polar coordinate system,

$$-j\omega\mu_0 d\vec{A^H} = \Big[-\frac{j\omega\mu_0}{4\pi r} \vec{J} d\Sigma_1 \Big] \exp(jkb \sin \theta \cos \overline{\phi' - \phi}$$

$$+ jkz \cos \theta - jkr). \qquad (4.8)$$

$$\frac{1}{j\omega\epsilon_0} \text{ grad div } d\vec{A^H} = \Big[\frac{j\omega\mu_0}{4\pi r} r J_r d\Sigma_1 \Big]$$

$$\exp\{jkb \sin \theta \cos \overline{\phi'} - \phi + jkz \cos \theta - jkr\} \qquad (4.9)$$

neglecting all higher powers of $(1/r)$

$$- \text{curl } d\vec{A^E} = \Big[\frac{-jk}{4\pi r} (\vec{\theta} M_\phi - \vec{\phi} M_\theta) d\Sigma_1 \Big]$$

$$\exp\{jkb \sin \theta \cos \phi' - \phi + jkz \cos \theta - jkr\} \qquad (4.10)$$

neglecting all higher powers of $(1/r)$ like $(1/r^2)$, $(1/r^3)$, etc.

Let $u' = kb \sin \theta$.

Substituting (4.8), (4.9) and (4.10) in (4.7), $\vec{E}_p$ is obtained as

$$\vec{E}_p = \frac{-jb}{4\pi r} \int\limits_{z=0}^{l} \int\limits_{\phi'=0}^{2\pi} \left[\vec{\theta}\,(\omega\mu_0 J_\theta + kM_\phi) \right.$$

$$+ \vec{\phi}\,(\omega\mu_0 J\phi - kM_\theta) \Big] \exp\{ju'\cos(\phi' - \phi)$$

$$+ jkz\cos\theta - jkr\} \, d\phi' dz. \tag{4.11}$$

Using the relations (4.4) for J_θ, J_ϕ, M_θ, M_ϕ

$$\vec{E}_P = \frac{-jb}{4\pi r} \int\limits_{\phi'=0}^{2\pi} \left[\vec{\theta}\,\{(-\omega\mu_0\sin\theta)\,C_2 + kC_1\cos(\phi' - \phi)\} \right.$$

$$+ \vec{\phi}\,\{k\cos\theta\sin(\phi' - \phi)\,C_1\} \Big] \exp\{ju'\cos(\phi' - \phi)\} \, d\phi'$$

$$\times \exp(-jkr) \int\limits_{z=0}^{l} \exp(-j\beta z)\exp(jkz\cos\theta)\,dz. \tag{4.12}$$

Let

$$x = l/2\,(\beta - k\cos\theta).$$

Then

$$\int\limits_{0}^{l} \exp\{jkz\cos\theta - j\beta z\}\,dz$$

$$= \int\limits_{0}^{l} \exp\{-j(\beta - k\cos\theta)\}z\,dz$$

$$= l\exp(-jlx)\left[\frac{\sin lx}{lx}\right]. \tag{4.13}$$

On substituting (4.13) in (4.12), the expression for $\vec{E}_p$ simplifies to

$$\vec{E}_P = \left(\frac{-jb}{4\pi r}\right) l\exp\{-j(lx + kr)\}\left[\frac{\sin lx}{lx}\right]$$

$$\times \left[\vec{\theta}\,\Big\{kA\,\frac{P(h)}{Y_0(u)}\Big\}\,2\pi j J_1(kb\sin\theta) \right.$$

$$+ \omega\mu_0\sin\theta\,\frac{j\omega\epsilon_1}{h}\,bA\,\frac{P'(h)}{Y_0(u)}\,2\pi J_0(kb\sin\theta) \Big]. \tag{4.14}$$

Setting

$$\frac{AP(h)}{Y_0(u)} = E_0$$

$$\left.\begin{array}{c} \\ \\ \end{array}\right\}$$ (4.15)

$$\frac{P'(h)}{hP(h)} = f(h)$$

$$\vec{E}_P \mid = \left(\frac{blk}{2}\right)\left(\frac{\sin lx}{lx}\right)\left(\frac{E_0}{r}\right) \exp\{-j(lx + kr)\}$$

$$\times [J_1(kb\sin\theta) + kb\epsilon_r f(h) J_0(kb\sin\theta)]. \tag{4.16}$$

Since

$$h = h_1 - jh_2 = h_1\left[1 - \frac{jh_2}{h_1}\right]$$

$$\cong h_1, \quad \text{since} \quad h_2/h_1 \ll 1$$

$$f(h) = f(h_1 - jh_2) \cong f(h_1).$$

Hence the radiated field due to the cylindrical dielectric surface of the antenna is

$$\vec{E}_{PS1} = \vec{\theta}\left\{\frac{blk}{2}\right\}\left(\frac{E_0}{r}\right)\left\{\frac{\sin\frac{l}{2}(\beta - k\cos\theta)}{\frac{l}{2}(\beta - k\cos\theta)}\right\} \exp\left\{-jl\frac{(\beta - k\cos\theta)}{2}\right\}$$

$$\times [\exp\{-jkr\}][J_1(kb\sin\theta) + kb\sin\theta\ \epsilon_r f(h_1)$$

$$\times J_0(kb\sin\theta)]. \tag{4.17}$$

4.2. *Field due to the Free End of the Antenna* (Σ_2)

When considering the radiation from the free end of the rod, the two tangential components to be considered are E_p and $H_{\phi'}$. These two components exist and have values given below at $Z = 1$. The coordinate system employed for this purpose is shown in Fig. 1.

$$E_\rho = \frac{-j\beta h}{h} A \frac{P'(\xi)}{Y_0(u)}$$

$$\left.\begin{array}{c} \\ \\ \end{array}\right\}$$ (4.18)

$$H_{\phi'} = \frac{-j\omega\epsilon_1 b}{h} A \frac{P'(\xi)}{Y_0(u)}$$

where

$$P'(\xi) = J_0'(\xi) Y_0(u) - J_0(u) Y_0'(\xi).$$

The unit vector perpendicular to the free end is in the z-direction.

$$\vec{J} = \vec{z} \times \vec{\phi}' H\phi' = -\vec{\rho} J_\rho = \vec{\rho} \, \frac{j\omega\epsilon_1 b}{h} \, A \, \frac{P'(\xi)}{Y_0(u)}$$

$$\vec{M} = -\vec{z} \times \vec{\rho} E_\rho = -\vec{\phi}' M_{\phi'} = \vec{\phi}' \, \frac{j\beta b}{h} \, A \, \frac{P'(\xi)}{Y_0(u)}. \tag{4.19}$$

By transforming the cylindrical coordinate system to the sph rical co-ordinate sys.em (see Table I) $\vec{J}$ and $\vec{M}$ can be written as

$$\vec{J} = \{\vec{r}(\sin\theta\cos\phi' - \phi) + \vec{\theta}(\cos\theta\cos\phi' - \phi)$$

$$+ \vec{\phi}(\sin\phi' - \phi)\} \left\{ A \, \frac{j\omega\epsilon_1}{h} \, b \, \frac{P'(\xi)}{Y_0(u)} \right\}. \tag{4.20}$$

$$\vec{M} = \{\vec{r}(-\sin\theta\sin\phi' - \phi + \vec{\theta}(-\cos\theta\sin\phi' - \phi)$$

$$+ \vec{\phi}(\cos\phi' - \phi)\} \left\{ A \, \frac{j\beta b}{h} \, \frac{P'(\xi)}{Y_0(u)} \right\}. \tag{4.21}$$

TABLE I

Transformation of co-ordinates

	r	θ	ϕ
ρ	$\sin\theta\cos(\phi' - \phi)$	$\cos\theta\cos(\phi' - \phi)$	$\sin(\phi' - \phi)$
ϕ'	$-\sin\theta\sin(\phi' - \phi)$	$-\cos\theta\sin(\phi' - \phi)$	$\cos(\phi' - \phi)$
Z	$\cos\theta$	$-\sin\theta$	0

The distance 'r_1' beween an element of area $d\Sigma_3 = \rho d\rho d\phi'$ on the free end and the distant point is given by

$$r_1 = r - \rho\sin\theta\cos(\phi' - \phi). \tag{4.22}$$

The vector potentials due to $\vec{J}$ and $\vec{M}$ are determined, and substituting these vector potentials in the expression for the radiated field, one obtains

$$\vec{E}_{Pe} = \left[\frac{kb}{4\pi rh} \right] [\vec{\theta}(\beta + k\cos\theta \, \epsilon_r)\cos(\phi' - \phi) + \vec{\phi}(\beta\cos\theta + k\epsilon_r)$$

$$\times \sin{(\phi' - \phi)} \exp{(-jkr)}] \left[\int_{\phi'=0}^{2\pi} \int_{\rho=a}^{b} \rho A \frac{P'(h\rho/b)}{Y_0(u)} \right.$$

$$\left. \times \exp{\{jk\rho \sin\theta \cos{(\phi' - \phi)}\}} \, d\rho d\phi' \right]. \tag{4.23}$$

After simplification, this reduces to

$$\vec{E}_{Pe} = \frac{kb}{4\pi rh} A \frac{1}{Y_0(u)} \int_{\rho=a}^{b} \rho P'\left(\frac{h\rho}{b}\right) \{\vec{\theta}(\beta + k \cos\theta \, \epsilon_r)$$

$$\times \exp{(-jkr)} [2\pi j J_1(k\rho \sin\theta)]\} \, d\rho. \tag{4.24}$$

Making use of Lommel's Integral formula, this can be further simplified. The final expression for the radiated field from the free end is

$$\vec{E}_{Pe} = \vec{\theta}j \left\{ \frac{bk}{2} \right\} \left(\frac{E_0}{r} \right) \left[\frac{\beta + k \cos\theta \, \epsilon_T}{\frac{h^2}{b^2} - k^2 \sin^2\theta} \right] \exp{(-jkr)}$$

$$\times \left[J_1(kb \sin\theta) + k \sin\theta \frac{1}{hP(h)} \{bP'(h) J_0(kb \sin\theta) \right.$$

$$\left. - aS(u) J_0(ka \sin\theta)\} \right]$$

where

$$S(u) = J_1(u) Y_0(u) - J_0(u) Y_1(u). \tag{4.25}$$

5. THE RESULTANT RADIATED FIELD

The resultant radiated field is obtained by adding (4.17) and (4.24) in proper phase

$$\vec{E}_P = \vec{E}_{PS1} + \vec{E}_{Pe}. \tag{5.1}$$

Adding (4.17) and (4.24) vectorially, we have

$$|\vec{E}_P|^2 = |\vec{E}_{PS1}|^2 + |\vec{E}_{Pe}|^2 - 2 |\vec{E}_{PS1}| |\vec{E}_{Pe}| \sin lx$$

where

$$x = \left(\frac{\beta - k \cos\theta}{2} \right). \tag{5.2}$$

Equation (5.2) expresses the radiated power as a function of the azimuthal angle ' θ '.

6. Gain of the Antenna

Besides the radiation pattern, the gain of the antenna is of equal interest to an antennal engineer. Makimoto, Sueta, and Nishimura[12] have obtained an expression for the gain of a dielectric rod aerial excited in HE_{11} mode. Wilkes[2] has also worked out an expression for the gain of a dielectric rod aerial.

By definition, the absolute gain of an antenna is the ratio of the radiated power flow per unit solid angle in the direction of maximum radiation to the average power flow per unit solid angle of an isotropic radiator with the same power input.

The radiated power flow per unit solid angle in the direction of maximum radiation is given by

$$\frac{1}{2\eta_0} \mid E_P \mid^2_{max} R^2$$

where $\eta_0 = 120\pi$ is the intrinsic impedance of free space. The average power flow per unit solid angle is $P/4\pi$ where P is the total power flow, in the dielectric-coated conducting cylinder excited in TM_{01} mode, in the direction of propagation.

Hence, the gain G is given by

$$G = \frac{R^2 \mid E_P \mid^2_{max}/2\eta_0}{P/4\pi} \tag{6.1}$$

$\mid E_P \mid^2$ is calculated and is given by equation (5.2) and the power P is given by[11]

$$P = [\epsilon_r N(h) + L(g)] P_0 \tag{6.2}$$

Hence

$$G = \frac{\mid E_P \mid^2_{max}}{60P} . \tag{6.2}$$

Gain G in

$$db = 10 \log_{10} \left[\frac{\mid E_P \mid^2_{max}}{60P} \right] . \tag{6.3}$$

7. EXPERIMENTAL DETERMINATION OF THE RADIATION PATTERN

The experimental set up used for the pattern measurement is shown in the form of a block schematic diagram in Fig. 2. The receiving antenna
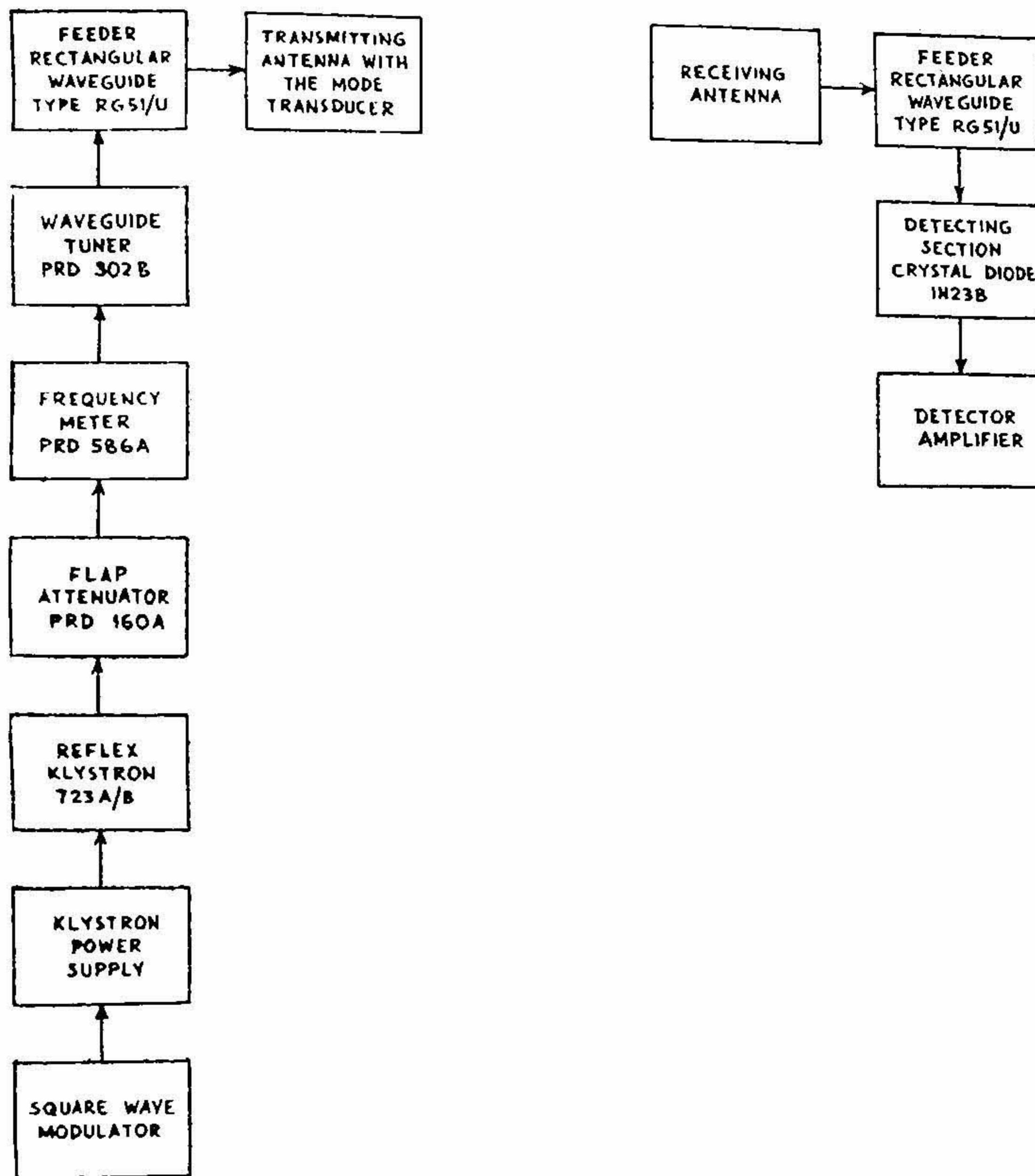

FIG. 2. Block schematic diagram of the set up used for the measurement of the radiation pattern.

is a pyramidal horn fixed so that the axis of the horn is in line with the axis of the transmitting antenna. The antenna under test is connected to the terminating end of the feeder, with the mode transducer. The mast in the
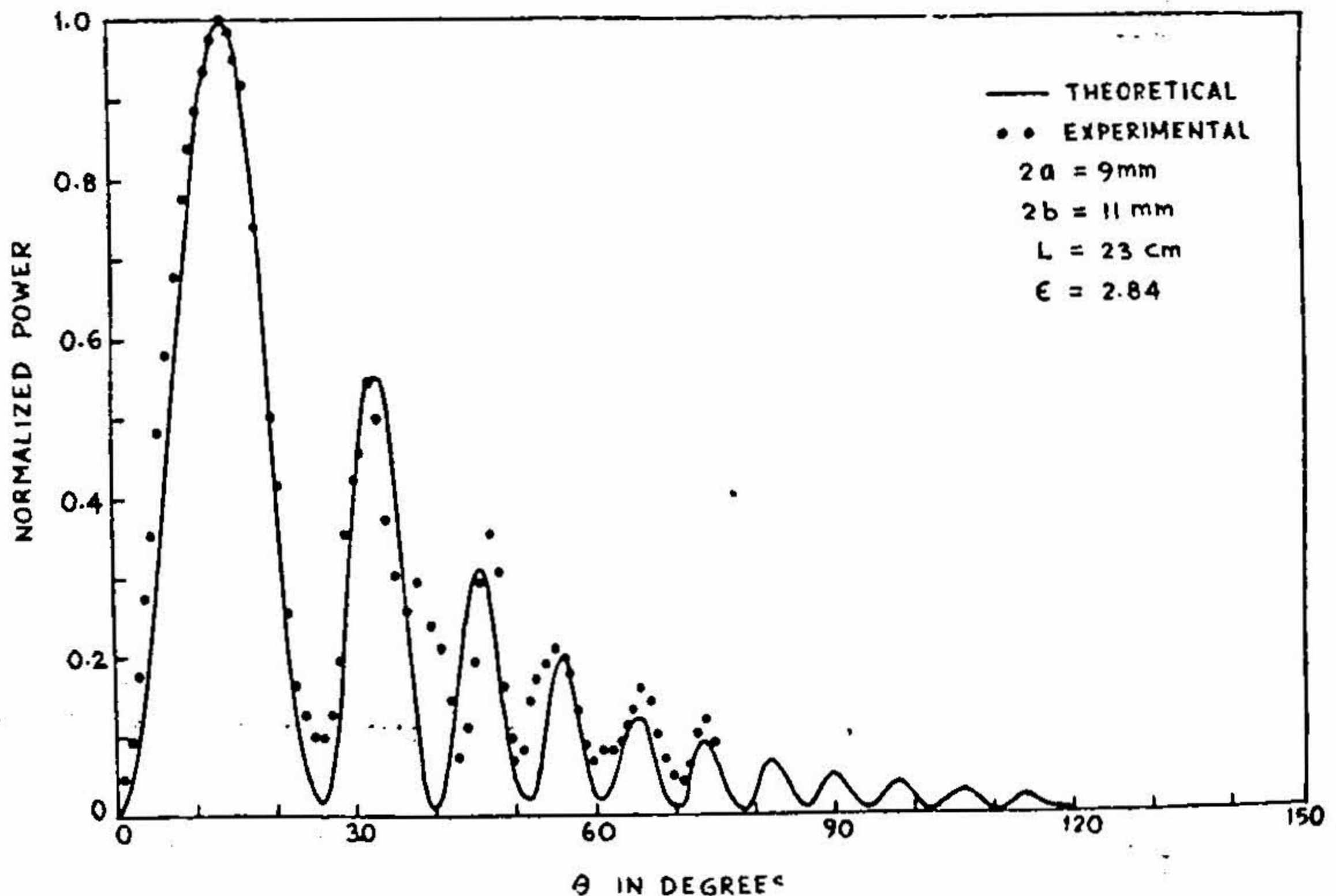
transmitting station which carries the transmitting antenna is rotated degree by degree and the detected output is noted. A plot of the power with the azimuthal angle gives the radiation power pattern.

The radiation pattern is symmetric about the axis and is characterized by a null in the forward direction. There are a few side lobes with varying positions and intensities.

8. Measurement of Gain

The gain of the aerial is found by a comparison method. Some standard antenna whose gain is known is chosen to be the reference antenna. A 19 db pyramidal horn is chosen as the reference antenna for comparison purposes. First, the reference antenna is connected to the waveguide section of the transmitter circuit. The maximum reading of the received power is noted down in the microammeter. Let this reading be 'P_1' μ Amps. Since the gain of the antenna is known, the input power to the horn can be found out from the formula

$$\text{Gain } (G)_{db} = 10 \log_{10}\left(\frac{P_1}{P}\right) \tag{8.1}$$

THEORETICAL
EXPERIMENTAL
$2a = 9$ mm
$2b = 11$ mm
$L = 23$ cm
$\epsilon = 2.84$

Fig. 3. Comparative study of the radiation pattern (thin dielectric coatings).

where P is the input power to the pyramidal horn. When the antenna whose gain is to be measured is connected to the waveguide with the mode transducer, the power at the input terminals of the antenna is equal to $\eta_L P$ where η_L is the a launching efficiency of the mode transducer. The maximum reading in the microammeter is noted when the antenna with the mode transducer is connected in place of the reference antenna. Let this reading be called $(P_2)\,\mu$ Amps. Then the gain of the antenna is given by

$$G = 10 \log_{10}\left(\frac{P_2}{\eta_L P}\right). \tag{8.2}$$

The launching efficiency of the mode transducer is experimentally determined by measuring the scattering coefficients using Desch amps method[15]. The value of the measured lauching efficiency of the mode transducers used is around 70%.

TABLE II

Comparative study of the radiation patterns—(A) Thin dielectric coatings

Material = Polythene $2a = 12\cdot7$ mm $2b = 16$ mm $\epsilon_t = 2\cdot25$

| L (cm)		Major lobe		Positions of side lobes in degrees and their intensities in db relative to the major lobe in brackets
		Position	Beam-width	
10	Theoretical	24	21	54 ($-6\cdot25$); 75 ($-8\cdot98$); 92 ($-11\cdot22$); 112 ($-16\cdot11$)
	Experimental	24	21	52 ($-6\cdot2$); 72 ($-7\cdot96$)
13	Theoretical	20	18	46 ($-5\cdot11$); 64 ($-8\cdot49$); 78 ($-9\cdot73$); 91 ($-11\cdot7$)
	Experimental	20	18	46 ($-5\cdot08$); 63 ($-8\cdot54$)
16	Theoretical	18	15·5	40 ($-3\cdot96$); 56 ($-7\cdot31$); 68 ($-9\cdot4$); 80 ($-10\cdot1$)
	Experimental	18	15·5	40 ($-3\cdot98$); 58 ($-7\cdot21$); 67 ($-10\cdot7$)
20	Theoretical	14	13·5	34 ($-2\cdot6$); 48 ($-5\cdot73$); 60 ($-7\cdot83$); 70 ($-9\cdot13$).
	Experimental	13·5	13·5	32 ($-2\cdot9$); 46·5 ($-5\cdot45$); 58 ($-8\cdot54$)
27	Theoretical	28	7	12 ($-0\cdot234$); 40 ($-2\cdot645$); 50 ($-4\cdot74$); 58 ($-6\cdot495$)
	Experimental	28	10	11 ($-0\cdot2$); 39 ($-3\cdot01$); 47 ($-5\cdot85$)
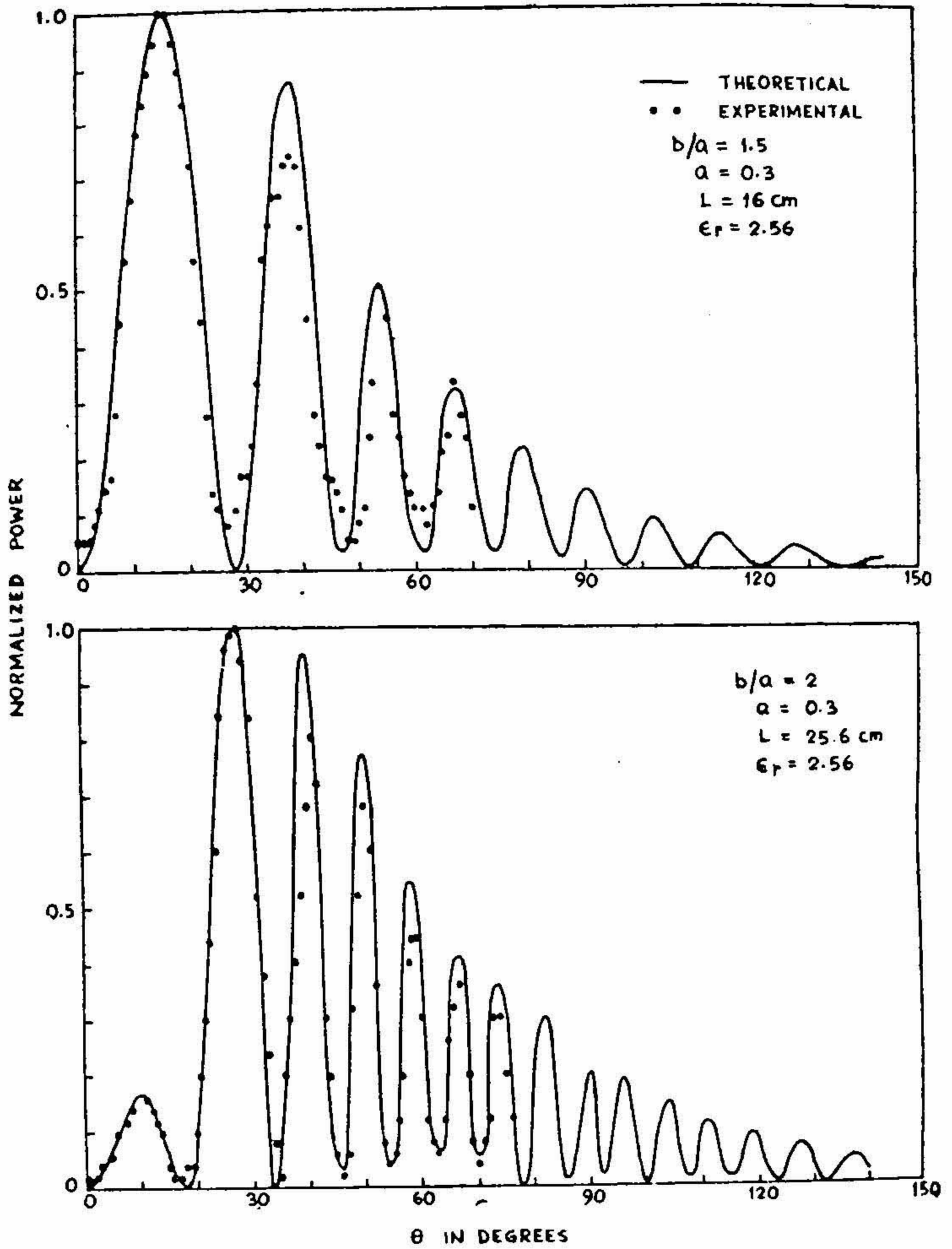
Fig. 4. Comparative study of the radiation pattern (thick dielectric coatings).

9. COMPARISON OF THE THEORETICAL AND EXPERIMENTAL RADIATION PATTERNS AND GAIN

Figs. 3–6 show a comparison between the calculated and measured radiation patterns. Fig. 3 corresponds to the case when the dielectric coating is thin. Figs. 4, 5 and 6 show the comparison when the coating is thick. Tables II and III show the comparative study of the radiation patterns when the dielectric coating is thin and thick respectively.
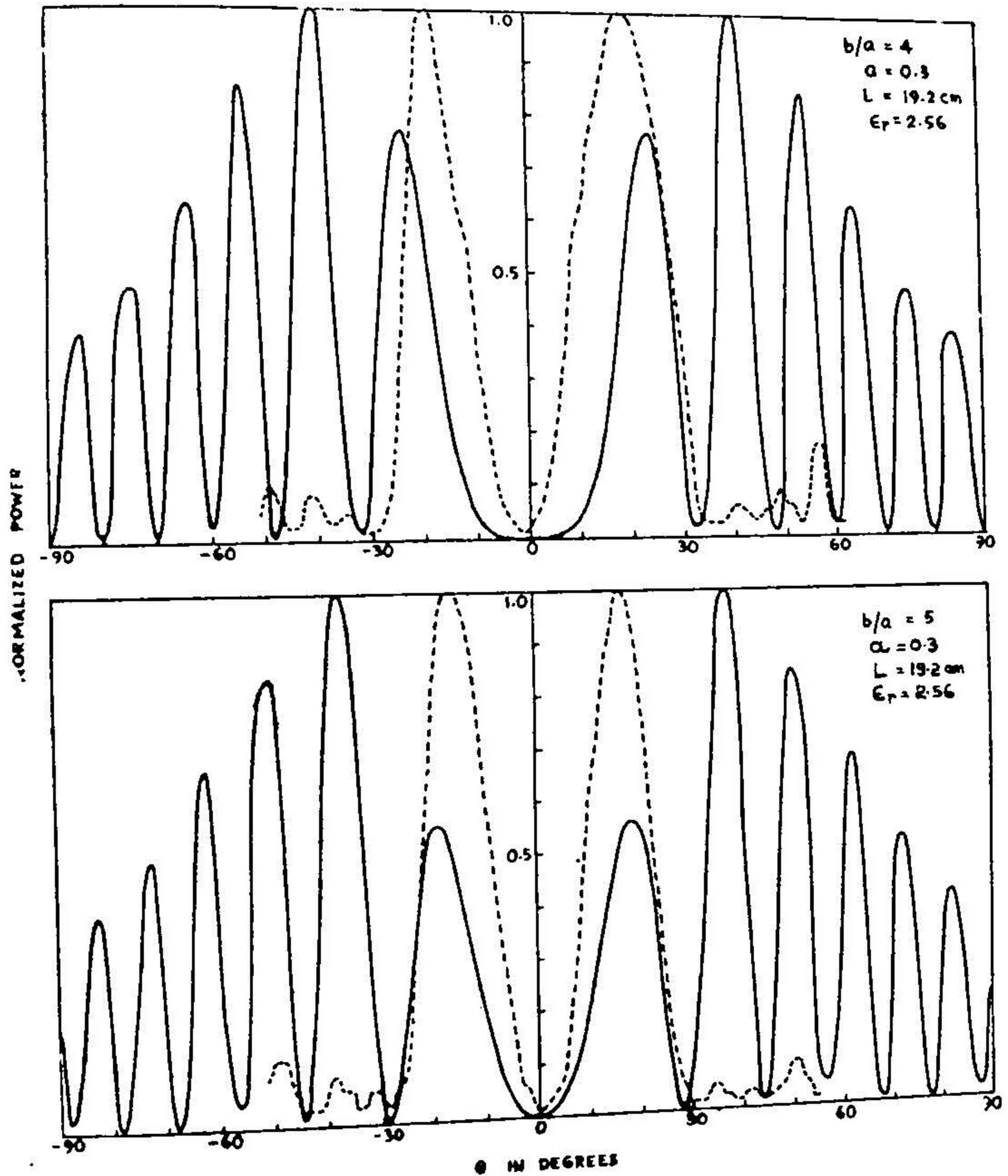

FIG. 5. Comparative study of the radiation pattern (thick dielectric coatings).
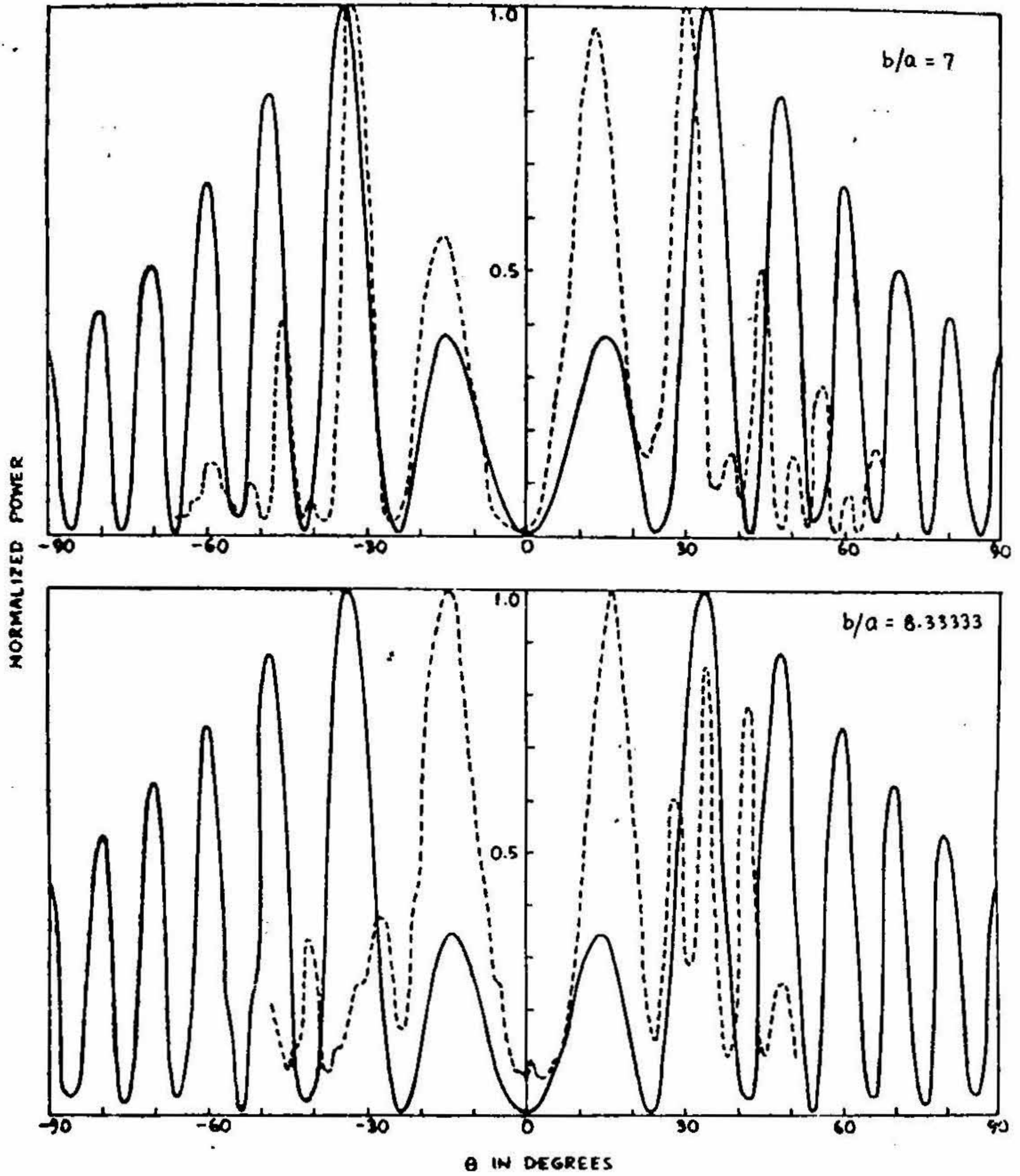——Calculated ;....Measured,

Fig. 6. Comparative study of the radiation pattern (thick dielectric coatings).
——Calculated;....Measured.

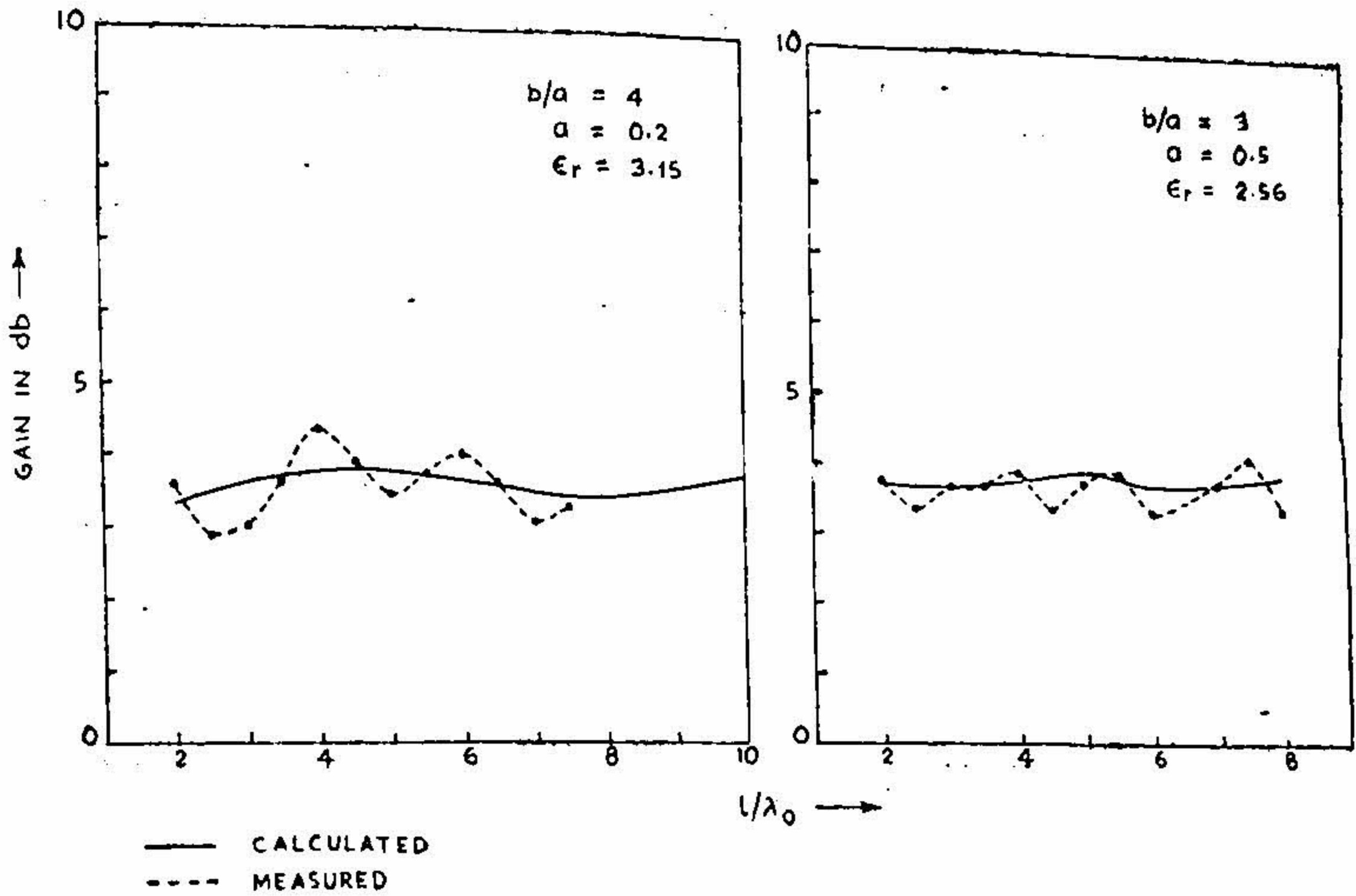$a=0\cdot3$ cm, $\epsilon_r=2\cdot56$, $L=19\cdot2$ cm.

FIG. 7. Comparative study of variation of the gain with the length of the antenna.

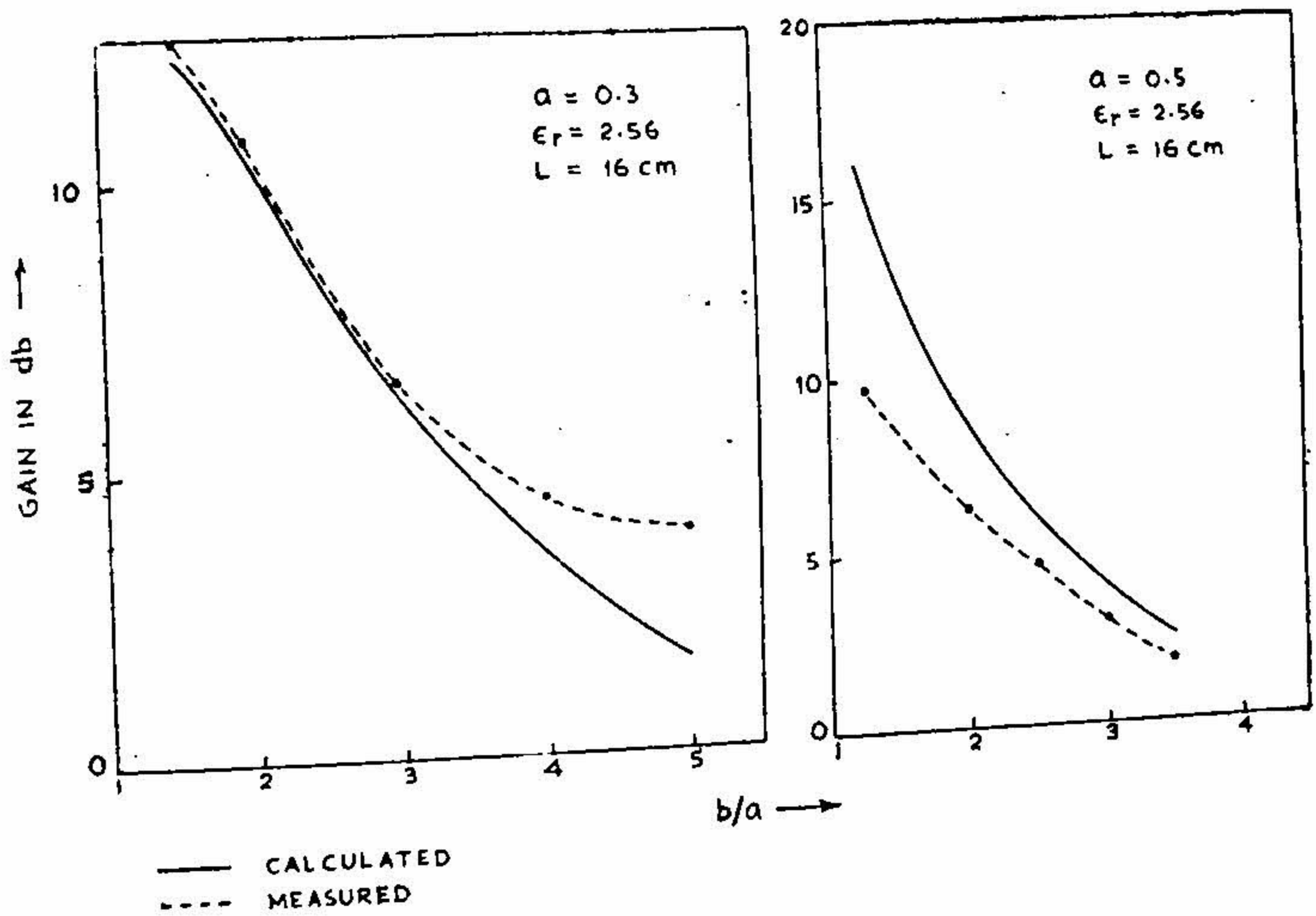FIG. 8. Comparative study of the variation of gain with b/a ratio.

Table III

Comparison of the radiation patterns—(B) Thick dielectric coatings

L (cm)	$2a$ (mm)	$2b$ (mm)		Major lobe		Positions and intensities of side lobes
				Position	Beamwidth	
25·6	10	12·5	Theoretical	12	11	30 (− 0·93); 42 (− 3·42); 52 (− 5·394); 60 (− 7·34); 68 (− 8·86); 76 (− 9·788)
			Experimental	12	10	30 (− 1·94); 42 (− 3·01); 52 (− 4·437); 60 (− 6·02); 69 (− 7·212)
16	10	15	Theoretical	34	10·5	12 (− 5·19); 50 (− 2·35); 64 (− 4·29); 76 (− 5·845); 88 ( )
			Experimental	34	10	12·5 (− 3·46); 50 (− 1·55); 63 (− 3·325); 75 (− 7·696)
16	6	9	Theoretical	16	14	38 (− 0·525); 54 (− 2·92); 68 (− 4·94); 80 (− 6·58); 90 (− 8·386)
			Experimental	15	13	38 (− 1·337); 54 (− 2·92); 67 (− 4·75)
25·6	6	12	Theoretical	28	8	10 (− 7·699); 40 (− 0·029); 50 (− 0·692); 58 (− 1·605); 66 (− 3·872); 74 (− 4·413); 82 (− 5·143); 90 (− 6·778)
			Experimental	28	8	9 (− 7·959); 41 (− 0·0969); 50 (− 1·675); 58·5 (− 3·565); 67 (− 4·437); 75 (− 5·229)

TABLE III (*Contd.*)

L (cm)	2a (mm)	2b (mm)		Major lobe		Positions and intensities of side lobes
				Position	Beamwidth	
19·2	6	24	Theoretical	40	7·5	24 (— 1·13); 54 (— 0·7017); 64 (— 1·965); 74 (— 3·236)
			Experimental	19	16	40 (— 12·2); 49 (— 10·7); 56 (— 7·447)
19·2	6	30	Theoretical	38	8	18 (— 2·52); (50 — 0·733); 62 (— 1·686); 72 (— 2·925)
			Experimental	17	13	35 (13·01); 50 (—10·458)
19·2	6	42	Theoretical	34	8	14 (— 4·288); 48 (— 0·799); 60 (— 1·759); 70 (— 2·936)
			Experimental	32·5	6·5	16 (— 1·229); 45 (— 3·495); 56 (— 5·376)
19·2	6	50	Theoretical	34	8	14 (— 4·585); 48 (— 0·567); 60 (— 1·294); 70 (— 1·9993)
			Experimental	16	10·5	28 (— 0·218); 34 (— 0·0655); 42 (— 1·051); 48 (— 6·021)

Gain.—A comparison is made between the calculated and measured values of gain. It is observed that conductors with thin dielectric coatings are good radiators and their values of gain are high. Table IV gives the calculated and measured values of gain for thin dielectric coatings.

In the case of thick dielectric coatings, the variation of the gain with the length is shown in Fig. 7. Fig. 8 shows the variation of gain with b/a ratio. The agreement between the theory and experiment is satisfactory in these cases.

Table IV

Calculated and measured values of gain

Sl. No.	Material	2a (mm)	2b (mm)	L (cm)	Calculated gain (G db)	Measured gain (db)
1	· Polythene	12·7	16	10	16·2	16·17
		12·7	16	13	16·767	16·721
		12·7	16	20	16·493	16·464
		12·7	16	27	15·676	15·611
2	Polythene	19	24	13·5	17	16·95
		19	24	16	16·44	16·52
		19	24	17·5	16	16·01
3	PVC	9	11	16	16·21	16·232
		9	11	23	16·23	16·28
		9	11	29·5	15·54	15·611
4	PVC	4	6	16	12·67	12·637
5	PVC	3	5	30	11·853	11·644

10. Discussion and Conclusions

The theoretical radiation characteristics like the position and beam-width of the major lobe, positions and intensities of side lobes agree well with the experiment for thin dielectric-coated conducting cylinders. The calculated gain of the antenna shows good agreement with the experiment for a thin dielectric coating. For a thickly coated conductor, the results of the experimental investigations deviate with the corresponding theoretical results *after a certain coating thickness is exceeded.* The reasons for the deviation can be any one of the following:

(i) when the dielectric coating becomes very thick, the surface wave tends to be a loosely bound surface wave;

(ii) there may be an interference between two or more waves in the direction of propagation;

(iii) a leaky wave may be generated which propagates at an angle to the axis of the guiding structure;

(iv) higher order modes may be present;

(v) As the ratio b/a increases, the major lobe of the radiation pattern of the finite length antenna moves away from the axis of the antenna, similar to the theoretical results obtained by Chung-Yu-Ting[17] for an infinitely long dielectric-coated metal antenna. More details of the above investigations are reported in (16).

11. ACKNOWLEDGEMENTS

REFERENCES

1. Watson, R. B. and Horton, C. W.   The radiation patterns of dielectric rods—experiment and theory. *Jour. Appl. Phys.*, 1948, **19**, 661–670.

2. Wilkes, G.   ..   Wavelength lenses. *Proc. I.R.E.*, February 1948, **36**, 206–212.

3. Horton, C. W., Karal, F. C. and McKinney, C. M.   On the radiation patterns of dielectric rods of circular cross-section—the TM_{01} Mode. *Jour. Appl. Phys.*, December 1950, **21**, 1279–1283.

4. Chatterjee, R. and Chatterjee, S. K.   Some investigations on dielectric rod aerials—Part I. *Jour. Ind. Inst. Sci.*, 1956, **38 B**, 93–103.

5. ———————   ..   Some investigations on dielectric rod aerials—Part III. *Ibid.*, 1957, **39 B**, 143–155.

6. Brown, J. and Spector, J. O.   The radiating properties of end-fire aerials. *Proc. I.E.E.* 1957, **104 B**, 27–34.

7. Ramanujam, H. R. and Chatarjee, R.   Some investigations on dielectric rod aerials—Part V. *Jour Ind. Inst. Sci.*, 1962, **44**, 164–202: Part VI, pp. 203–218.

8. Fradin, A. Z.   ..   *Microwave Antennas*, (Pergamon Press).

9. Silver, S.   ..   *Microwave Antenna Theory and Design*, McGraw-Hill Book Co., Inc.

10. Kiely, D. G.   ..   *Dielectric Aerials*, Metheuen's Monograph.

11. James, J. R.   ..   Theoretical investigation of cylindrical dielectric rod antennas *Proc. I.E.E.*, March 1967, **114** (3), 309–319.

12. Sueta, T., Nishimura, S. and Makimoto, T.   A study on the radiation mechanism of dielectric rod antennas and the new types with high gain. *Elect. and Comm. Japan*, 1965, **48**, 228.

13. Chatterjee. R. and Chandrakaladhara Rao, T.

Dielectric-coated circular cylindrical metal antennas excited in the *TM* symmetric mode at microwave frequencies. Under publication in *The Indian Journal of Radio and Space Physics.*

14. Chandrakaladhara Rao, T. and Chatterjee, R.

Circular cylindrical dielectric-coated metal rod excited in the symmetric TM_{01} mode. Part I. Surface-wave propagation characteristics. *Jour. Ind. Inst. Sci.* 193, 55, 193–231.

15. Deschamps. G. A.   ..

Determination of reflection coefficient and insertion loss of a waveguide junction. *Journ. Appl. Phys.*, August 1953, 24, 1046–1050.

16. Chandrakaladhara Rao, T.

Surface wave and radiation characteristics of a circular cylindrical dielectric-coated metal rod. *PhD. Thesis,* Indian Institute of Science, Bangalore-12, submitted July 1972.

17. Ting, Ching-Yu   ..

Infinite cylindrical dielectric-coated antenna. *Radio Science,* March 1967, 2(3), 325–335.